ELSEVIER

Journal of Molecular Catalysis A: Chemical 172 (2001) 97–116

JOURNAL OF MOLECULAR CATALYSIS A: CHEMICAL

www.elsevier.com/locate/molcata

A theoretical and experimental study about the effect of different organosilanes on immobilization of $(n\text{BuCp})_2ZrCl_2$ on pre-treated SiO_2

M.L. Ferreira [a,*], P.P. Greco [b], J.H.Z. dos Santos [b], D.E. Damiani [a]

[a] *PLAPIQUI-UNS-CONICET — Camino La Carrindanga, Km 7, 717-8000 Bahía Blanca, Argentina*
[b] *Instituto de Química — UFRGS, Avenue Bento Gonçalves 9500, 91509-900 Porto Alegre, Brazil*

Received 13 September 2000; accepted 8 March 2001

Abstract

This work presents the results of theoretical and experimental characterization of supported $(n\text{BuCp})_2ZrCl_2$ on organosilanes pre-treated SiO_2. Several possibilities are analyzed and considered as an attempt to explain the observed zirconocene loadings, catalyst performance in ethylene polymerization and resulting polymer properties of these supported zirconocenes. The effect of silica pre-treatment with Ph_3SiCl, Me_3SiCl and Me_2HSiCl on the immobilization of $(n\text{BuCp})_2ZrCl_2$ was modeled. The main considered aspects were the role of the surface concentration of the organosilanes, the presence or absence of residual chlorine and the possibility of interactions between the organosilanes and the zirconocene. All these facts might afford different surface species at the impregnation step prior to the MAO activation during the polymerization reaction.

Keywords: Organosilanes; Immobilization; Polymerization

1. Introduction

The impact of metallocene catalysts extends beyond simple olefin polymerization. The development of new polyolefins inaccessible by classical Ziegler–Natta polymerization has afforded increasingly importance to such class of single-site catalysts. It is believed that within 10 years 20% of world's polyethylene production will be based on metallocene catalysts. Two major drawbacks have retarded their industrial application: the huge amounts of coactivator methylaluminoxane (MAO) necessary to achieve high activity and stability; and the desirable heterogeneization, in order to adapt the present polymerization plants, which run with heterogeneous catalysts (drop-in technology). The heterogeneization is also important to avoid reactor fouling, polymer swelling and to afford better control of polymer morphology.

Several silica-supported metallocene catalysts have been reported in [1–4]. They may be grouped into two types: MAO mediated and directly supported routes.

Metallocene heterogeneization studies indicate that impregnation directly on silica is not a suitable method to achieve high productivity. There are several reports about the effect of the silica pre-treatment temperature on the ethylene polymerization activity ([5]) and the surface metal (Zr) loading ([6]). In case of directly supported, several modifiers can be added to the pre-treated silica in order to avoid undesirable secondary reactions of the metallocene,

* Corresponding author.

1381-1169/01/$ – see front matter
PII: S1381-1169(01)00129-7

mainly bimolecular deactivation that leads to very low productivity.

Most of the studies employing chemically modified silica concern improving monomer access to active sites through the use of a spacer between the silica surface and the metallocene species [1–3]. Soga et al. [7] prepared supported catalysts, in which silica was initially modified with Me_2SiCl_2, followed by MAO, prior to Cp_2ZrMe_2 impregnation. Such systems were active in ethylene polymerization using common alkylaluminium cocatalysts. Immobilization of Cp_2ZrMe_2 on silica chemically modified with Me_3SiCl was claimed to yield a high activity catalyst in ethylene polymerization, even in absence of any cocatalyst. Dos Santos et al. [8] have reported the increase of activity in ethylene polymerization using Ph_3SiCl, Me_3SiCl and Me_2HSiCl as silica modifiers, in a supported $(n\text{BuCp})_2ZrCl_2$ catalyst. The main function of the organosilane was found to be an horizontal spacer to keep apart metallocene species on the silica surface. However, the effect seems to be more complex, since the resulting polyethylene polydispersity decreases and also the crystallinity in case of using high amounts of Ph_3SiCl. The activities were equal or even higher than those exhibited by homogeneous catalyst in selected conditions.

Taking into account the results of [8], the objective of this wok is to perform a more careful characterization of the systems resulting from the chemical modification of thermally treated silica surface with three organosilanes (Ph_3SiCl, Me_3SiCl and Me_2HSiCl).

The effect of these in the grafting of a zirconocene ($(n\text{BuCp})_2ZrCl_2$) in ethylene polymerization was analyzed. The main aspects considered here were the role of the surface concentration of the organosilanes, the presence or absence of residual chlorine and the possibility of interactions between the organosilanes and the zirconocene. The nature of the different potential generated surface species prior to the MAO activation step at the polymerization reaction was analyzed, too.

2. Experimental

2.1. Materials

Silica Grace 948 ($255\,m^2\,g^{-1}$) was activated under vacuum ($P < 10^{-4}$ mbar) for 16 h at 723 K. The support was then cooled to room temperature under dynamic vacuum and stored under dried argon. MAO (gently supplied by Witco, 10.0 wt.% toluene solution, average molar mass $900\,g\,mol^{-1}$), $(n\text{BuCp})_2ZrCl_2$ (Witco), Ph_3SiCl (Aldrich), Me_3SiCl (Aldrich), Me_2SiHCl (Merck) were used without further purification. Ethylene, provided by COPESUL Co., and argon were deoxygenated and dried through columns of BTS (gently supplied by BASF) and activated molecular sieve (13 Å) prior to use. Pure grade toluene and methyl dichloride were deoxygenated and dried by standard techniques before use.

2.2. Preparation of supported catalysts

All grafting experiments were performed under inert atmosphere using the Schlenk technique. Organosilicon-modified silicas were prepared by impregnating 1.0 g of activated silica Grace 948 with a toluene organosilicon solution, corresponding to 0.15–5.00 wt.% Si/SiO_2, at room temperature for 30 min. The solvent was removed by vacuum and then a toluene metallocene solution of $(n\text{BuCp})_2ZrCl_2$ corresponding to 1.5 wt.% Zr/SiO_2 was added and stirred for 1 h at 353 K. The slurry was then filtered through a fritted disk. The resulting solids were washed with $12\times\ 2.0\,cm^3$ of toluene and dried under vacuum for 4 h. An analogous procedure was employed in the immobilization of $(n\text{BuCp})_2ZrCl_2$ on bare SiO_2, but in this case the organosilicon impregnation step was suppressed. Resulting metal content were determined by Rutherford backscatering spectrometry (RBS) and are reported elsewhere [8].

2.3. X-ray photoelectron spectroscopy (XPS)

The spectra were obtained on a PHI 5600 Esca System (Φ Physical Electronics), using monochromated Al Kα radiation (1486.6 eV). Acquisition was carried out at room temperature in high-resolution mode (23.5 eV pass energy). For the Cl 2p, Si 2p, and O 1s regions. The samples were mounted on an adhesive copper tape as thin films. Samples were prepared in a glove box, introduced into a transfer chamber and then evacuated at 10^{-6} Torr in 90 min using a turbomolecular pump. During data collection, an ion-getter pump kept the pressure in the analysis chamber under 10^{-9} Torr. Analysis area was 800 μm in diameter.

Each sample was analyzed at a 75° angle relative to the electron detector. For each of the XPS spectra reported, an attempt has made to deconvolute the experimental curve in a series of peaks representing photoelectron emission from atoms in different chemical environments. These peaks are described as a mixture of Gaussian (80%) and Lorentzian (20%) contributions to take instrumental error into account together with the characteristic shape of photoemission peaks.

2.4. Fourier transform infrared spectroscopy

Transmission Fourier transform infrared spectroscopy (FTIR) spectra were recorded on a Bomem MB-102 Spectrometer, (32 scans at a $4\,cm^{-1}$ resolution). The study was restricted to the mid-infrared region ($3800–2000\,cm^{-1}$) due to strong bulk absorption of silica at lower wavenumbers. The samples analyzed by this technique consisted of 25–35 mg of silica Aerosil pressed under 12 MPa into a self-supporting tablet ($\varnothing = 17$ mm) which was introduced into a Pyrex cell with CaF_2 windows. The unit was attached to a greaseless glass gas/vacuum handling system and the silica tablet was activated in situ under vacuum ($<10^{-4}$ mbar) at 723 K for 16 h. Organosilicon and $(n\text{BuCp})_2ZrCl_2$ impregnations were then conducted from a methyl dichloride solution. This solution contained an amount of organosilicon equivalent to that employed in the chemical modification of silica and/or an amount of zirconocene corresponding to those determined by RBS in catalysts prepared when silica Grace 948 was pre-treated at the same temperature. Methyl dichloride was employed instead of toluene because it is more easily removed by vacuum in the drying step. All spectra were recorded at room temperature.

2.5. Theoretical method

The semiempirical extended Hückel (EH) method [9] has been extensively applied to study of the electronic structure of molecules. In the present work we have employed a modified version of this method, ICONC, developed by Calzaferri et al. [10], which does not involve great computational effort. Although this method does not calculate representative absolute energies, it can be employed to predict qualitative trends in model system. ICONC has been applied to study the CH_3OH adsorption–oxidation process on V_2O_5 [11] and to the analysis of Ziegler–Natta and metallocene catalyst [12] and VO_x/Al_2O_3 catalyst [13]. Other details about EHMO calculation (parameters, considerations) can be found in the literature [10–13].

We want to emphasize that the main merit of the method is to provide valuable relative comparisons. The experimental results of FTIR have been taken account of to try of visualize the surface structures of silanes, especially in case of several options that arise from the reactions. Reaction energies alone might not always suffice to discriminate between different possible paths. No reaction paths are presented here. Only initial and final states have been considered in the calculations.

The reported ΔEs are calculated as the sum over the energies of the products minus the sum over the energies of the reactives for each reaction. In case of the obtained minimum in the distances O (support)–Si (organosilane) the energies are calculated as the energy of the reacted molecule on surface and the product evolved as gas (HCl) minus the support and the organosilane energies (at infinite distance each other).

2.6. SiO_2

The structure of amorphous silica is claimed to be similar to that of β-crystobalite [14,15]. The (1 0 0) and the (1 1 1) faces were considered as the most abundant exposed planes, being 85% (1 1 1) plane. The (1 0 0) face presents geminal OH groups, while isolated silanol groups are on the (1 1 1) face.

SiO_2(1 1 1) plane includes 50 H, 39 O and 26 Si. SiO_2(1 0 0) plane has 61 H, 30 O and 16 Si. The surfaces were considered thermally dehydrated, therefore, siloxane groups are present (see Figs. 1 and 2).

2.7. $(nBuCp)_2ZrCl_2$

The structures of substituted compounds like $(RCp)_2ZrCl_2$ divide into two distinct groups, illustrated schematically in Figs. 3 and 4. The model of this zirconocene was obtained from [16–18]. The zirconocene was modeled with all its atoms: 47 (see Fig. 5). Structure shown in Fig. 3 is adopted by compounds with bulky substitutents (R = *tert*-butyl) but in other cases, the structure shown in Fig. 4 is preferred

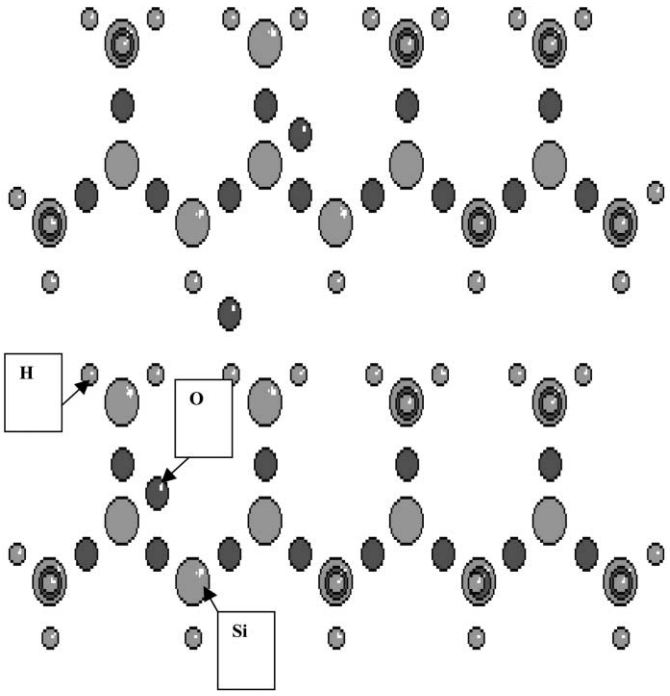

Fig. 1. SiO_2(1 1 1) plane.

with the substituents exactly or approximately eclipsed above and below the MCl_2 group. Considering the reaction of the chlorine with OH from surface as the preferred reaction of the selected zirconocene compound, we selected the structure depicted in Fig. 3 (Structure I). When it is alkylated or hydrogenated, the zirconocene changes its symmetry to a non-C_2 (see Fig. 6), with the chlorine far from the ciclopentadienyl groups, and it maintains the structure numbered I.

2.8. Silanes (Me_3SiCl, Me_2HSiCl, Ph_3SiCl)

All the silanes were modeled with all their atoms. The distance Si–Cl was 2.019 Å, Si–H was 1.48 Å, Si–C was selected as 1.875 Å (as in $Si(CH_3)_4$) [19]. In all cases, Si was considered tetrahedral and the angles were 109.5°. These distances were selected taking into account reported structural data from different silanes [20] (see Fig. 7).

2.9. Interaction organosilanes–silica

For both silica planes, several different reactions were evaluated. It is known that evolution of HCl takes place when chlorosilanes are fixed on SiO_2 [20] therefore, we modeled this reaction for all the silanes, obtaining the distances support–organosilane when minima were found. Besides, we evaluated the reaction of organosilanes with reactive siloxanes, that are known to be present in high concentration according to recent reports about silica chemical properties treated at temperatures higher than 473 K, but lower than 873 K [21,22]. In this case no evolution of gas is expected, only an addition reaction by siloxane rupture.

2.10. Interaction zirconocene–supported silanes

The capacity for the supported organosilanes to alkylate the zirconocene soluble in toluene was evaluated in case of methylated species on surface.

2.11. Interaction zirconocene–silica

The interaction of zirconocene with OH from both planes of silica was considered. Besides, the reaction with siloxane groups was evaluated.

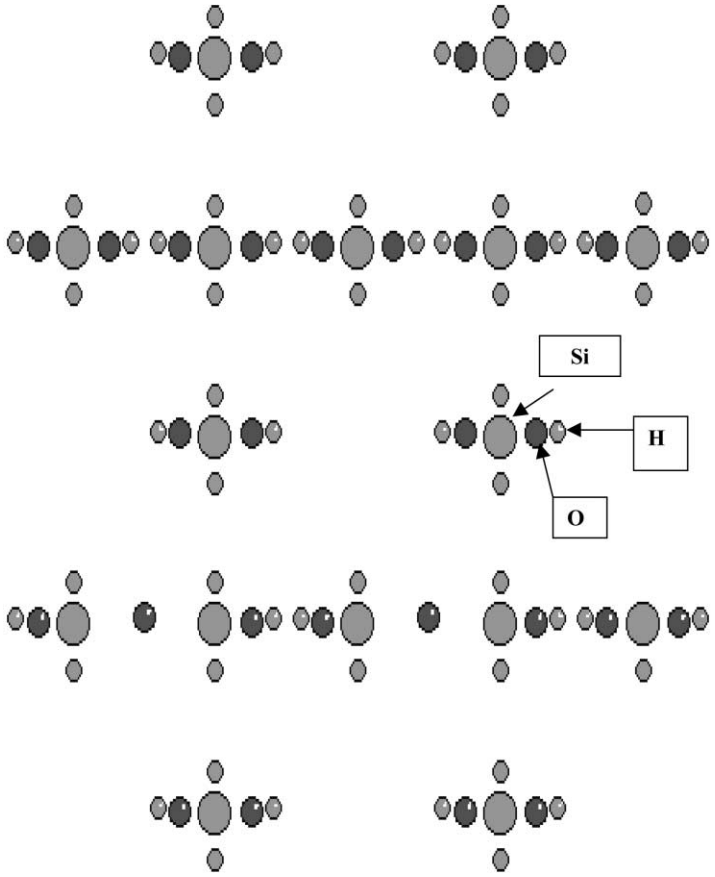

Fig. 2. $SiO_2(1\,0\,0)$ plane.

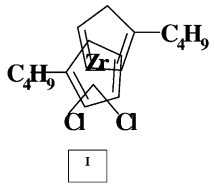

Fig. 3. Structure I of substituted, unbridged zirconocenes.

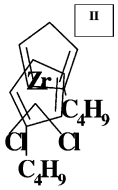

Fig. 4. Structure II of substituted, unbridged zirconocenes.

2.12. Interaction supported zirconocene–supported silanes

Several other possibilities were evaluated: exchange of Cl and methyl in case of supported methylated species ($SiMe_3$ or $SiHMe_2$) near a supported zirconocene and exchange of Cl by H in case of supported $SiHMe_2$ near a supported zirconocene.

2.13. The MAO model

The MAO model is a very short model that considers the presence of two kinds of methyls groups in tricoordinated Aluminium (more acidic than Al in other coordinations): internal and terminal methyl groups. The terminal methyl groups are reported to be the more reactive in zirconocene alkylation [21,22]. It includes

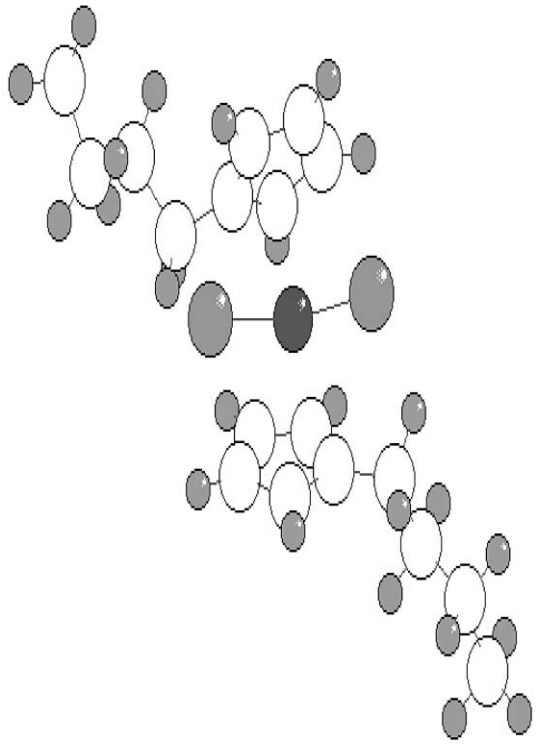

Fig. 5. Structure of $(n\text{BuCp})_2ZrCl_2$.

2 Al, 2 O, 3 methyl groups and 1 terminal H (see Fig. 8). The exchange of methyl by chlorine can be produced at the terminal methyl or in the internal one.

3. Results and discussion

3.1. Theoretical

3.1.1. SiO_2(1 1 1) (isolated)

3.1.1.1. Silanes. For this plane we considered the reaction of isolated OH and strained reactive siloxane groups. The organochlorosilane as a reactant with water produces organosilanes, which rapidly undergo condensation reaction to an organosiloxanol and an organosiloxane [20]. The silica is considered in our paper to be water free because of the high pre-treatment temperature. Therefore, this reaction can be ruled out in this case. The annealing of silica at temperatures up to about 773 K causes partial dehydroxylation, yielding strained, and hence, highly reactive siloxane groups [21,22].

With monofunctional organochlorosilanes, the following mechanism is the most likely [21,22]:

$$\equiv\text{Si–OH} + \text{XSiR}_3 \rightarrow \equiv\text{Si–O–SiR}_3 + \text{HCl} \quad (1)$$

3.1.1.2. Me_3SiCl. The most extensive studies on silica surface modification have been made with this compound. The maximum surface concentration of trimethylsilylgroups is about $4.0 \pm 0.5\,\mu\text{mol/m}^2$ on porous silicas of different origin and on non-porous finely dispersed as Aerosil [20]. With fully hydroxylated silicas only 50% of the total number of hydroxyl groups are able to take part in the reaction. Even with the closest packing of trimethylsilane (TMS) groups, the distances between two adjacent methyl groups correspond roughly to their Van der Waals radii of about 4 Å. Babkin and Kiselev [23] stated that even with maximum coverage residual hydroxyl groups still remain (see Fig. 9).

In fact the presence of TMS groups prevent the remaining OH groups from reacting. These coating defects are particularly important with bulky groups such as phenyl groups.

The mean distance between TMS groups has found to be 8 Å [20]. The mean molecular cross-sectional area is estimated to be $0.42\,\text{nm}^2$, which is twice that of OH group. The TMS surface, even at the densest coverage is an extended layer of thickness near 3.5 Å. The dispersion interactions of an adsorbate with the TMS layer are weak and might mainly be caused by

1. the saturated character of the methyl group; and
2. the large distance form the parent surface.

There is a lot of work on this topic [24]. From the reported data, impregnation temperatures as high as 723 K are necessary to achieve a complete coverage.

Under our experimental treatment temperature, probably the organosilane effective final coverage, after toluene washing, is low.

Since 1968 it is known that OH can exchange Chlorine. The paper of Hair and Hertl [25] shows that with monochlorosilane a first order kinetics is obtained when it reacts with Cab-O-Sil. For the authors this fact means that the free hydroxyl groups have about the same reactivity. This does not hold for the first 10–15% of the reaction, when a high activity is found. The monofunctional silane shows a residual Cl content not present in the original Cab-O-Sil. The high reactivity is due to the exchange reaction.

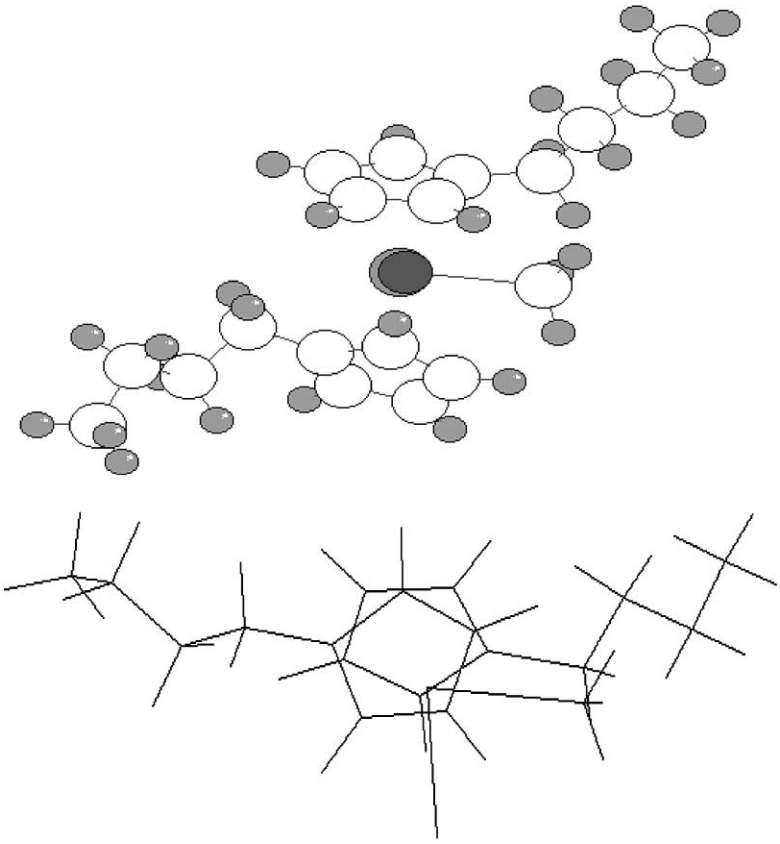

Fig. 6. Structure of (nBuCp)$_2$ZrClX (X different from Cl).

Table 1 (reactions 2–7) presents the results about the interaction with the (1 1 1) silica plane. The reaction with siloxane (Table 1, reaction 7) is the most favorable one. Evolving HCl is the preferred reaction way for the $SiMe_3$ fixation (Table 1, reaction 1 and Fig. 10). Exchange of Chlorine by OH from the surface is a favored process (see Table 1, reaction 4).

3.1.1.3. Me_2SiHCl. The reactions 8–14 (Table 1) present the possible interactions of this silane with silica surface. The Reaction with siloxane groups is the most favored (reactions 10, 11, 13 and 14, Table 1). The fixation of this silane to the surface is mainly by evolution of HCl (reaction 8). Neither methane (reaction 9, Table 1) nor water (reaction 12) are possible reaction products. Exchange of Cl by OH from the surface is probable, too (reaction 10, Table 1). The reaction product with siloxane is depicted in Fig. 11.

3.1.1.4. Ph_3SiCl. In case of this organochlorosilane, there is no evidence of chlorine remaining from the impregnation step, even at high impregnation temperatures as 473–357 K [20]. Therefore, the siloxane rupture and Chlorine exchange reaction can be ruled out in this case.

Reaction 15 (Table 1) presents the only possible way to fix Ph_3Si.

3.1.1.5. $(nBuCp)_2ZrCl_2$. Reactions 16 and 17 (Table 2) show the possible reactions with surface. The reaction with OH groups is favored (see Fig. 14).

3.1.2. SiO_2(1 0 0) (geminal)

For this plane we considered the reaction of geminal groups for two final structures on silica(1 0 0) plane provided by the reaction of Me_3SiCl (see Figs. 12 and 13, Reactions 18 and 19, Table 2) and Me_2SiHCl

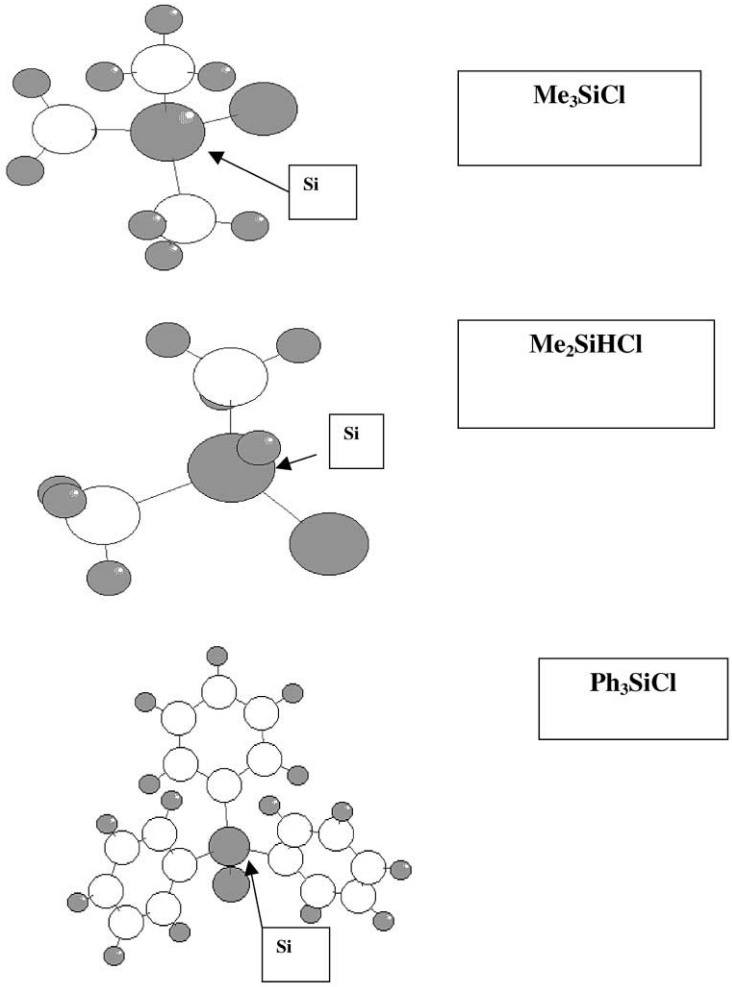

Fig. 7. Silanes structures Me_3SiCl, Me_2H SiCl and Ph_3SiCl.

(reactions 20–23, Table 2). There is no difference in case of considering the structure square planar instead of tetrahedral for the silanes.

Reaction evolving HCl for Me_3SiCl is the most probable (see reaction 18, Table 2), whereas evolution of HCl and H_2 is the most favored for Me_2SiHCl (reaction 22, Table 2).The fixation of chlorine as SiMeCl group is possible with this silane (reaction 21, Table 2).

3.1.2.1. $(nBuCp)_2ZrCl_2$. The zirconocene reacts preferentially with the (1 0 0) plane (see reactions 25 and 16, Table 2), leading to inactive zirconocene precursors.

See Figs. 14 and 15 to compare the final structure of the zirconocene on both surfaces ((1 1 1) and (1 0 0)).

From this set of reactions several points can be discussed.

1. The several possible ways to find chlorine present on the surface are: by the OH–chlorine exchange and in the case of Me_3SiCl and Me_2HSiCl, by reactions where chlorine remains on surface (the siloxane rupture, and reactions on (1 0 0) plane).

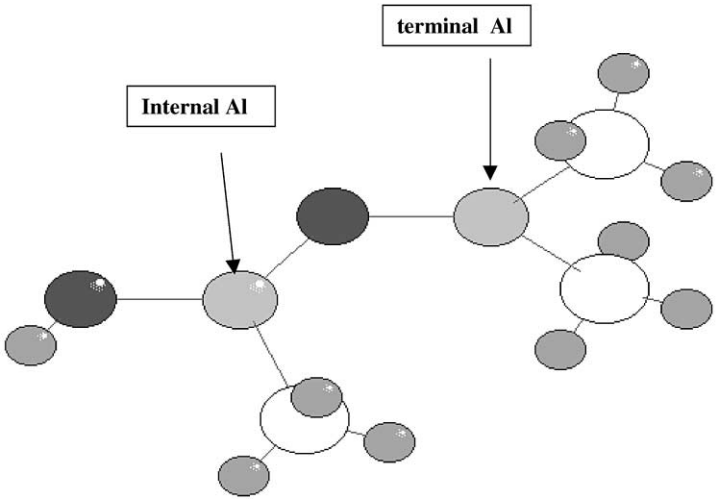

Fig. 8. Short MAO model.

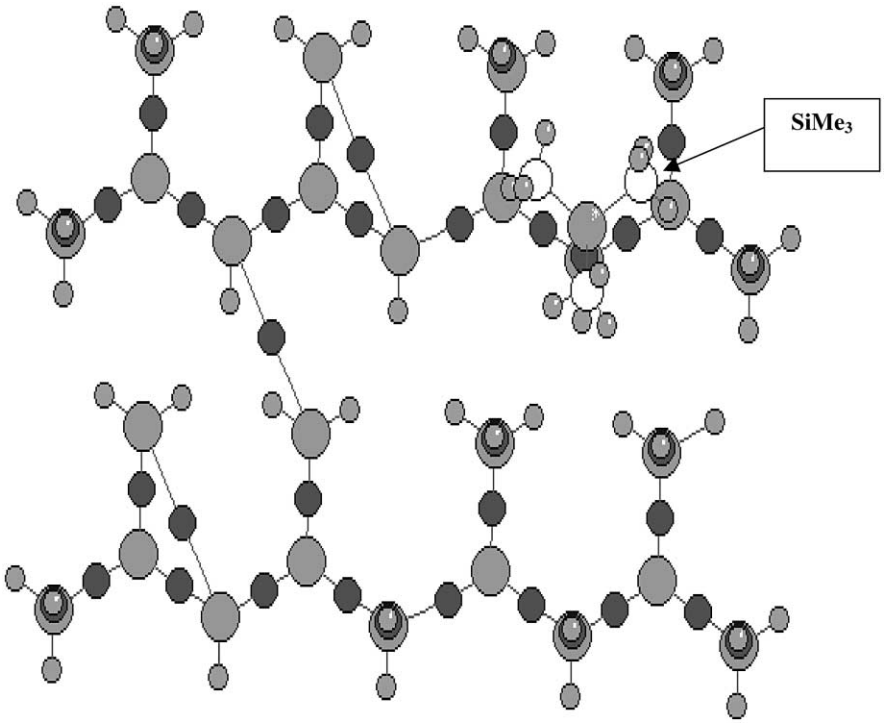

Fig. 9. Silica(1 1 1)–O–$SiMe_3$.

Table 1
Reactions of silanes on SiO_2(1 1 1)

Reaction number	Schema	ΔE (eV)	Figure
SiO_2(1 1 1) (isolated) Me_3SiCl			
(2) Evolution of HCl	Silica(1 1 1)–OH + $ClSiMe_3$ → HCl + silica(1 1 1)–O–$SiMe_3$; distance Si–($SiMe_3$)–O– (SiO_2) = 2.75 Å	−1.48	9
(3) Evolution of methane	Silica(1 1 1)–OH + $ClSiMe_3$ → CH_4 + silica(1 1 1)–O–$SiMe_2Cl$	+0.40	
(4) Exchange of chlorine by OH from surface	Silica(1 1 1)–OH + $ClSiMe_3$ → silica(1 1 1)–Cl + $OHSiMe_3$	−1.07	
(5) Reaction of $OHSiMe_3$ with strained siloxane	Silica(1 1 1)≡Si–O–Si≡silica(1 1 1) + $OHSiMe_3$ → silica(1 1 1)≡$SiOH^*$ $SiMe_3O$–Si≡silica(1 1 1)	−1.80	
(6) Evolution of water	Silica(1 1 1)–OH + $OHSiMe_3$ → silica(1 1 1)–O–$SiMe_3$ + H_2O	+0.14	
(7) Reaction Me_3SiCl-siloxane	Silica(1 1 1)≡Si–O–Si≡silica(1 1 1) + $ClSiMe_3$ → silica(1 1 1)≡$SiCl^*$ $SiMe_3O$–Si≡silica(1 1 1)	−2.35	10
Me_2SiHCl			
(8) Evolution of HCl	Silica(1 1 1)–OH + $ClSiHme_2$ → HCl + silica(1 1 1)–O–$SiHMe_2$; distance Si($SiHMe_2$)–O(SiO_2) = 3.05 Å	−1.34	
(9) Evolution of methane	Silica(1 1 1)–OH + $ClSiHMe_2$ → CH_4 + silica(1 1 1)–O–$SiHMe_2Cl$	+0.34	
(10) Exchange of chlorine by OH from surface	Silica(1 1 1)–OH + $ClSiHMe_2$ → silica(1 1 1)–Cl + $OHSiHMe_2$	−2.55	
(11) Reaction of $OHSiHMe_2$ with strained siloxane	Silica(1 1 1)≡Si–O–Si≡silica(1 1 1) + OHSiHMe2 → silica(1 1 1)≡$SiOH^*$ HMe_2SiO–Si≡silica(1 1 1)	−0.69	
(12) Evolution of water	Silica (1 1 1)–OH + $OHSiHMe_2$ → silica(1 1 1)–O–$SiHMe_2$ + H_2O	+1.49	
(13) Reaction $ClSiHMe_2$-siloxane	Silica(1 1 1)≡Si–O–Si≡silica(1 1 1) + $ClSiHMe_2$ → silica(1 1 1)≡$SiCl^*$ HMe_2SiO–Si≡silica(1 1 1)	−2.72	
(14) Reaction $ClSiHMe_2$-siloxane	Silica(1 1 1)≡Si–O–Si≡silica(1 1 1) + ClSiHMe2 → silica(1 1 1)≡SiH^* $ClMe_2SiO$–Si≡silica(1 1 1)	−2.15	11
Ph_3SiCl			
(15) Evolution of HCl	Silica(1 1 1)–OH + $ClSiPh_3$ → HCl + silica(1 1 1)–O–$SiPh_3$; distance Si($SiPh_3$)–O(SiO_2) = 2.35 Å	−3.42	

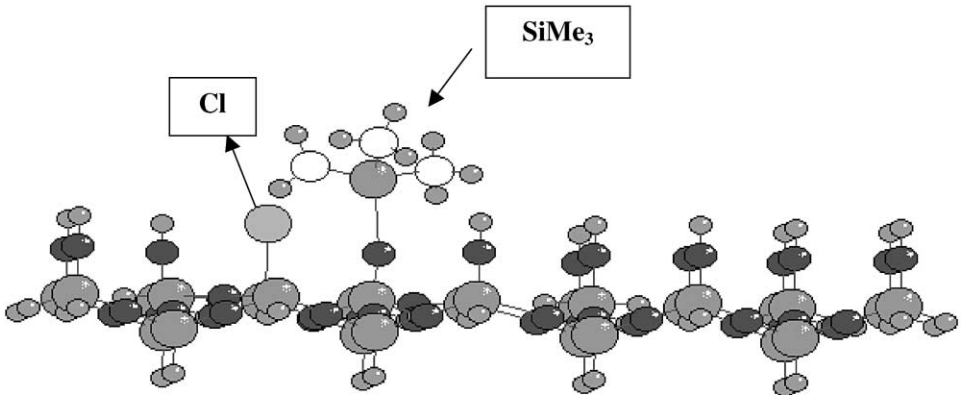

Fig. 10. Silica(1 1 1)≡SiCl* $SiMe_3O$–Si≡silica(1 1 1).

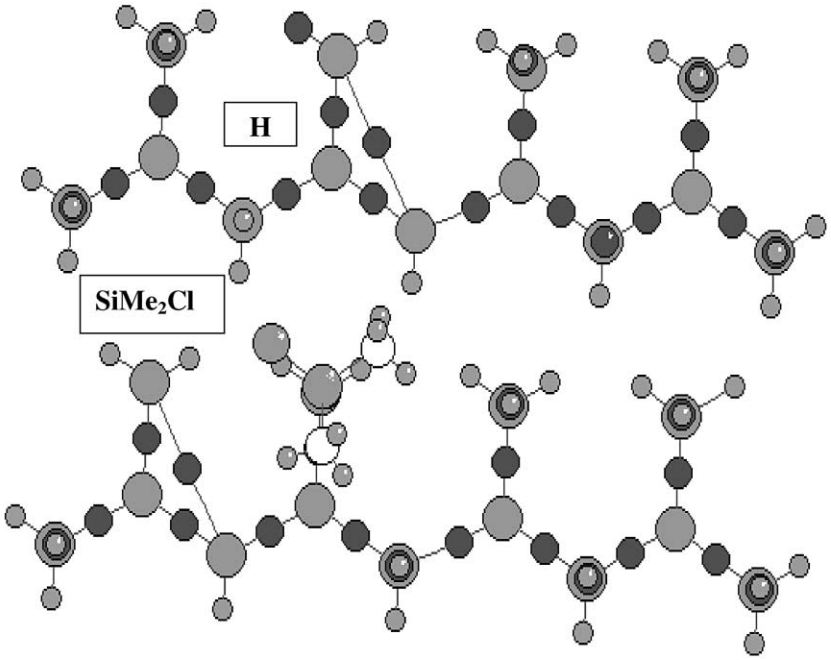

Fig. 11. Silica(1 1 1)≡SiH* $ClMe_2SiO$–Si≡silica(1 1 1).

2. In the case of Me_2HSiCl several hydrogenated surface species can be present at the preparation step.
3. Methylated species are found on the surface with Me_3SiCl and Me_2HSiCl.

In order to evaluate the possibility that supported organosilanes can alkylate (or hydrogenate) the ziconocene in the toluene solution several other reactions were taken into account.

3.2. Reactions of zirconocene with the supported silanes

3.2.1. SiO_2(1 1 1)

Tables 2 and 3 present the results of calculations of these interactions (reactions 26–34). Reactions 26–30 of Table 2 show the results of reaction of the zirconocene dichloride. Reactions 31–34 of Table 3

Table 2
Reactions of silanes and zirconocene on $SiO_2(1\,1\,1)$ and $SiO_2(1\,0\,0)$[a]

Reaction number	Schema	ΔE (eV)	Figure
$(n\text{BuCp})_2ZrCl_2$			
(16) Evolution of HCl	Silica(1 1 1)–OH + $(n\text{BuCp})_2ZrCl_2$ → silica(1 1 1)–OZr(nBuCp)$_2$Cl + HCl	−4.78	14
(17) Reaction with siloxane	Silica(1 1 1)≡Si–O–Si≡silica(1 1 1) + $(n\text{BuCp})_2ZrCl_2$ → silica(1 1 1)≡SiCl* (nBuCp)$_2$ZrCl–OSi≡silica(1 1 1)	−3.88	
$SiO_2(1\,0\,0)$ (geminal) Me_3SiCl			
(18) Reaction with geminal silanols	Silica(1 0 0)$(OH)_2$+ $ClMe_3Si$ → silica(1 0 0)$(O)_2SiMe_2$ + HCl + CH_4; distance Si (silane)–O(SiO_2) = 2.47 Å	−1.79	12
(19) Reaction with geminal silanols	Silica(1 0 0)$(OH)_2$+ $ClMe_3Si$ → silica(1 0 0)$(O)_2SiMeCl$ + $2CH_4$	−1.53	13
Me_2SiHCl			
(20) Reaction with geminal silanols	Silica(1 0 0)$(OH)_2$ + $ClMe_2HSi$ → silica(1 0 0)$(O)_2SiHMe$ + HCl + CH_4	−2.47	
(21) Reaction with geminal silanols	Silica(1 0 0)$(OH)_2$ + $ClMe_2HSi$ → silica(1 0 0)$(O)_2SiMeCl$ + CH_4 + H_2	−3.93	
(22) Reaction with geminal silanols	Silica(1 0 0)$(OH)_2$ + $ClMe_2HSi$ → silica(1 0 0)$(O)_2SiMe_2$ + ClH + H_2	−4.19	
(23) Reaction with geminal silanols	Silica(1 0 0)$(OH)_2$ + $ClMe_2HSi$ → silica(1 0 0)$(O)_2$Si HCl + $2CH_4$	−3.29	
Ph_3SiCl			
(24)	Silica(1 0 0)$(OH)_2$ + $ClPh_3Si$ → silica(1 0 0)$(O)_2SiPh_2$ + PhH + HCl	−4.85	
$(n\text{BuCp})_2ZrCl_2$			
(25) Reaction with geminal silanols	Silica (1 0 0)–$(OH)_2$ + $(n\text{BuCp})_2ZrCl_2$ → silica (1 0 0)–OZr(nBuCp)$_2$ + 2HCl	−5.25	15
Reactions of zirconocene with the supported silanes $SiO_2(1\,1\,1)$			
(26)	Silica(1 1 1)–O–$SiMe_3$ + $(n\text{BuCp})_2ZrCl_2$ → $(n\text{BuCp})_2ZrClCH_3$ + silica(1 1 1)–O–$SiMe_2Cl$	−0.037	
(27)	Silica(1 1 1)≡SiCl* $SiMe_3O$–Si≡silica(1 1 1) + $(n\text{BuCp})_2ZrCl_2$ → $(n\text{BuCp})_2ZrClCH_3$ + silica(1 1 1)≡SiCl* $SiMe_3O$–Si≡silica(1 1 1)	−0.024	
(28)	Silica(1 1 1)–O–$SiMe_2H$ + $(n\text{BuCp})_2ZrCl_2$ → $(n\text{BuCp})_2ZrClH$ + silica(1 1 1)–O–$SiMe_2Cl$	−3.92	
(29)	Silica(1 1 1)–O–$SiMe_2H$+ $(n\text{BuCp})_2ZrCl_2$ → $(n\text{BuCp})_2ZrClCH_3$ + silica(1 1 1)–O–SiMeHCl	−0.18	
(30)	Silica(1 1 1)≡SiCl* HMe_2SiO–Si≡silica(1 1 1) + $(n\text{BuCp})_2ZrCl_2$ → $(n\text{BuCp})_2ZrClH$ + silica(1 1 1)≡SiCl* $ClMe_2SiO$–Si≡silica(1 1 1)	−3.50	

[a] Interactions between zirconocene and supported silanes(I).

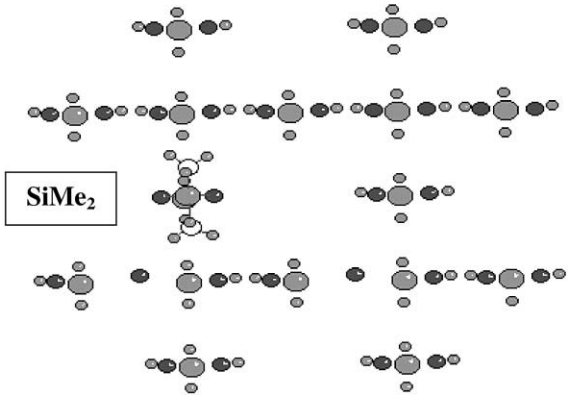

Fig. 12. Silica(1 0 0)$(O)_2SiMe_2$.

present the results of the interaction of modified zirconocenes (methylated, mono or di-hydrogenated) with supported silanes. From these results it is clear that the chlorine exchange by methyl (reactions 26, 27 and 29, Table 2) is not so favored as the exchange of chlorine by hydrogen (reactions 28 and 30, Table 2). Therefore, in case of Me_2HSiCl, the formation of mono (reactions 32 and 34, Table 3) and even di-hydrogenated species of Zr in the toluene solution (reaction 31, Table 3) can not be ruled out. The interaction of methylated zirconocene with the silica surface with HCl evolution is energetically favored (see reaction 33, Table 3).

The di-hydrogenated species produced by reaction 31 or 32 (Table 3) could suffer reaction with physisorbed silane, providing Zr–Si bonds, with methane or HCl evolution, and therefore, unable to be supported on silica.

3.2.2. Interaction supported zirconocene–supported silanes

This interaction was considered to take account of the different distribution of zirconocene when organosilanes are present as silica modifiers. Reactions 35–40 (Table 3) show the importance of enough room at surface to support efficiently the zirconocene. Compare Reactions 35 and 36 with 37 and 39. The exchange of chlorine by methyl groups is favored comparing it with the exchange of H (reactions 38 and 40, Table 3) (see Figs. 16 and 17).

3.2.3. SiO_2(1 0 0)

In the three situations considered (reactions 41–43, Table 3) the zirconocene is placed at 5 Å away from the Si of silane (see Fig. 17). It is clear that the zirconocene must be at longer distance than 5 Å to avoid steric hindrance in case of supported Ph_2Si.

In order to analyze the importance of the presence of chlorine at the silica surface, we performed some calculations about the possibility of exchange of chlorine from the surface with MAO. We used a short MAO model, with terminal and internal methyl groups.

Whatever the involved methyl group, the methyl (MAO)–chlorine (supported silane) exchange with the surface is claimed to be possible (see reactions 44–49, Table 3).

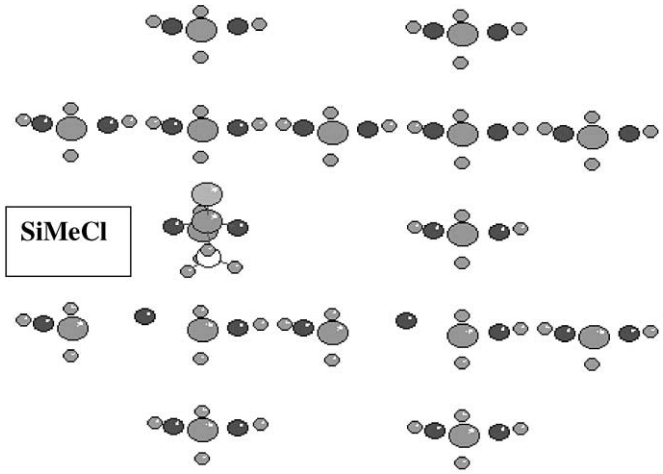

Fig. 13. Silica(1 0 0)$(O)_2SiMeCl$.

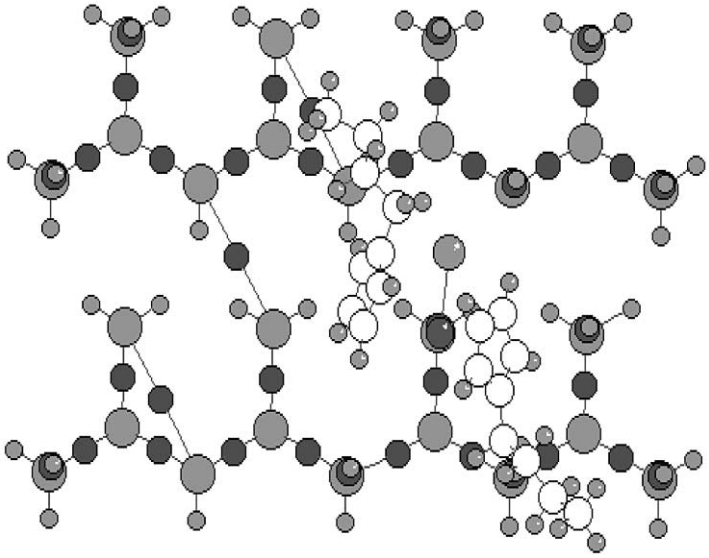

Fig. 14. Silica(1 1 1)–OZr(nBuCp)$_2$Cl.

3.3. Experimental characterization

Modifications on silica surface after each preparative step were monitored by in situ FTIR spectroscopy.

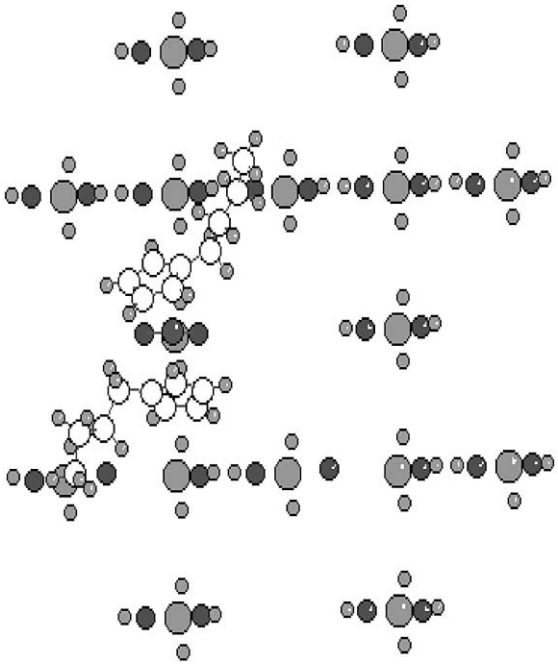

Fig. 15. Silica(1 0 0)–OZr(nBuCp)$_2$.

As an example, Fig. 18 presents some spectra concerning the different systems studied here.

Fig. 18a shows the spectrum of a silica surface activated under vacuum at 723 K. The sharp peak at 3747 cm^{-1} can be assigned to isolated, non-interacting silanol groups, while the very broad band centered about 3692 cm^{-1} is due to hydrogen bonded pairs or chains of silanols [26,27].

The immobilization of 1.0 wt.% Si/SiO_2 of Ph_3SiCl leads to a reduction of intensity of isolated SiOH band at 3747 cm^{-1}. Under such conditions, there is 16% intensity reduction, indicating that isolated OH groups were either consumed by the surface reaction or perturbed, since the appearance of a broad band centered at 3621 cm^{-1} is also observed (Fig. 18b). The impregnation of Ph_3Si groups is also accompanied by the appearance of three bands in the region of aromatic ν_{C-H}, corresponding to the stretching vibration of the phenyl groups: 3067, 3055 and 3016 cm^{-1} [28].

The impregnation of 3.0 wt.% Si/SiO_2 of Me_3SiCl (spectrum c of Fig. 18) leads to about 80% OH band intensity reduction (see Table 4). Stretching vibrations associated to CH_3 groups are observed at 2873 cm^{-1}.

In the case of 0.3 wt.% Si/SiO_2 Me_2SiHCl-modified silica, followed by impregnation of 0.12 wt.% Zr/SiO_2,

Table 3
Interactions between zirconocene and supported silanes(II)

Reaction number	Schema	ΔE (eV)	Figure
Reactions of zirconocene with the supported silanes SiO_2(1 1 1)			
(31)	Silica(1 1 1)–O–$SiMe_2H$ + (nBuCp)$_2$ZrClH → (nBuCp)$_2$ZrH_2 + silica(1 1 1)–O–$SiMe_2Cl$	−2.45	
(32)	Silica(1 1 1)–O–$SiMe_2$HSi–OH +(nBuCp)$_2$ZrH_2 → silica (1 1 1)–OsiMe_2HSi–OZr(nBuCp)$_2$H + H_2	−4.50	
(33)	Silica(1 1 1)–O–$SiMe_2$HSi–OH+(nBuCp)$_2$ZrClCH_3 → silica(1 1 1)–OSiMe_2HSi–OZr(nBuCp)$_2$$CH_3$ + HCl	−7.76	
(34)	Silica(1 1 1)–O–$SiMe_2$HSiOH + (nBuCp)$_2$ZrClH → silica (1 1 1)–$SiMe_2$HSi–OZr(nBuCp)$_2$H + HCl	−4.24	
Interaction supported zirconocene–supported silanes			
(35)	Silica(1 1 1)–O–$SiMe_3$+(nBuCp)$_2$ZrCl_2 → silica(1 1 1)–OZr(nBuCp)$_2$Cl···Me_3Si–O–silica(1 1 1) + HCl (zirconocene near $SiMe_3$)	+5.91	
(36)	Silica(1 1 1)–O–$SiMe_2$H+(nBuCp)$_2$ZrCl_2 → silica(1 1 1)–OZr(nBuCp)$_2$Cl···Me_2HSi–O–silica(1 1 1) + HCl (zirconocene near $SiMe_2$H)	+6.07	
(37)	Silica(1 1 1)–O–$SiMe_3$ +(nBuCp)$_2$ZrCl_2 → silica(1 1 1)–OZr(nBuCp)$_2$Cl···Me_3Si–O–silica(1 1 1) + HCl (zirconocene away 5 Å from $SiMe_3$)	−4.03	
(38)	Silica(1 1 1)–OZr(nBuCp)$_2$Cl···Me_3Si–O–silica(1 1 1) → silica(1 1 1)–OZr(nBuCp)$_2$$CH_3ClMe_2$Si–O–silica(1 1 1)	−7.77	16
(39)	Silica(1 1 1)–O–$SiHMe_2$ +(nBuCp)$_2$ZrCl_2 → silica(1 1 1)–OZr(nBuCp)$_2$Cl···Me_2HSi–O–silica(1 1 1) + HCl (zirconocene away 5 Å from $SiMe_3$)	−4.06	
(40)	Silica(1 1 1)–OZr(nBuCp)$_2$Cl···Me_2HSi–O–silica(1 1 1) → silica(1 1 1)–OZr(nBuCp)$_2$H···Me_2ClSi–O–silica(1 1 1) + HCl	−5.33	17
SiO_2(1 0 0)			
(41)	Silica(1 0 0)(O)$_2$SiMe_2Si(OH)$_{2+}$ + (nBuCp)$_2$ZrCl_{2-} → 2HCl + silica(1 0 0)SiMe_2Si(O)$_2$Zr(nBuCp)$_2$	−5.07	
(42)	Silica(1 0 0)(O)$_2$SiMeHSi(OH)$_2$ + (nBuCp)$_2$ZrCl_{2-} → 2HCl + silica(1 0 0)SiMeHSi(O)$_2$Zr(nBuCp)$_2$	−4.82	
(43)	Silica(1 0 0)(O)$_2$SiPh_2Si(OH)$_2$ + (nBuCp)$_2$ZrCl_2 → silica(1 0 0)(O)$_2$SiPh_2Si(O)$_2$Zr(nBuCp)$_2$ + 2HCl	+6.48	
Exchange Cl (surface)–MAO[a]			
(44)	Silica(1 1 1)–O–$SiMe_2Cl$ + MAO → silica(1 1 1)–O–$SiMe_3$ + MAOCl int	−1.18	
(45)	Silica(1 0 0)(O)$_2$SiMeCl + MAO → silica(1 0 0)(O)$_2$SiMe_2 + MAOCl int	−0.53	
(46)	Silica(1 1 1)–Cl + MAO → silica(1 1 1)–Me + MAOCl int	−0.48	
(47)	Silica(1 1 1)–O–$SiMe_2Cl$ + MAO → silica(1 1 1)–O–$SiMe_3$ + MAOCl terminal	−1.5	
(48)	Silica(1 0 0)(O)$_2$SiMeCl + MAO → silica(1 0 0)(O)$_2$SiMe_2 + MAOCl terminal	−0.85	
(49)	Silica(1 1 1)–Cl + MAO → silica(1 1 1)–Me + MAOCl terminal	−0.8	

[a] Exchange of Cl (from supported silanes) by methyl group of MAO.

only a reduction of ca. 13% of the initial SiOH band intensity is observed (Fig. 18d). In a previous study, we observed also a partial reduction of ν_{Si-H} (2155 cm^{-1}) band, suggesting that it be also partially consumed, besides the isolated silanol groups [8]. The reduction was of almost 35%. The four bands placed between 2962 and 2864 cm^{-1} correspond to asymmetric and symmetric ν_{C-H} in the CH_3 and CH_2 fragments of the nBu groups from the zirconocene catalyst. The decrease of the Si–H band can be related to the reaction of this silane with zirconocene in many ways (exchange of Cl from Zr–Cl by H from H–Si — see Eq. 28, Table 2). Other reactions are presented in equations 30–32 and 34.

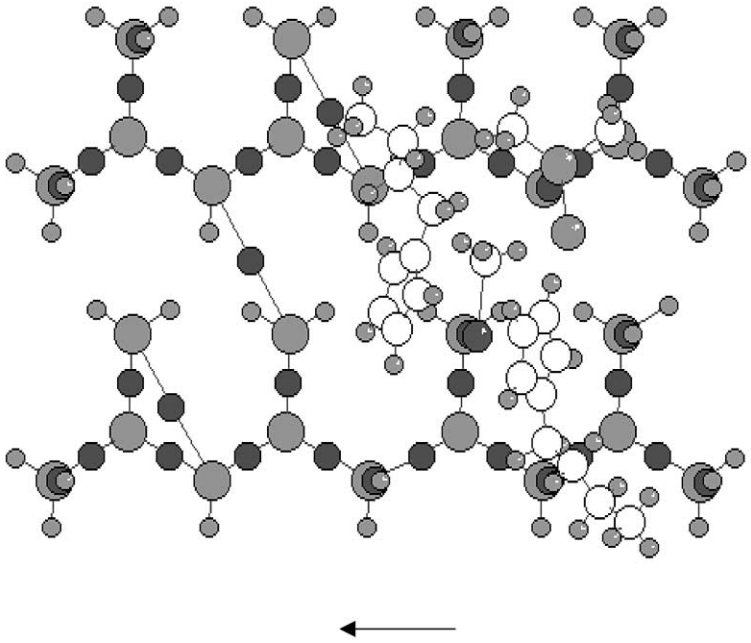

Fig. 16. Silica(1 1 1)–OZr(nBuCp)$_2$CH$_3$$\cdots$ClMe$_2$Si–O–silica(1 1 1) (near the zirconocene and the supported silane). The arrow shows the direction of shift of zirconocene to avoid repulsive inter actions.

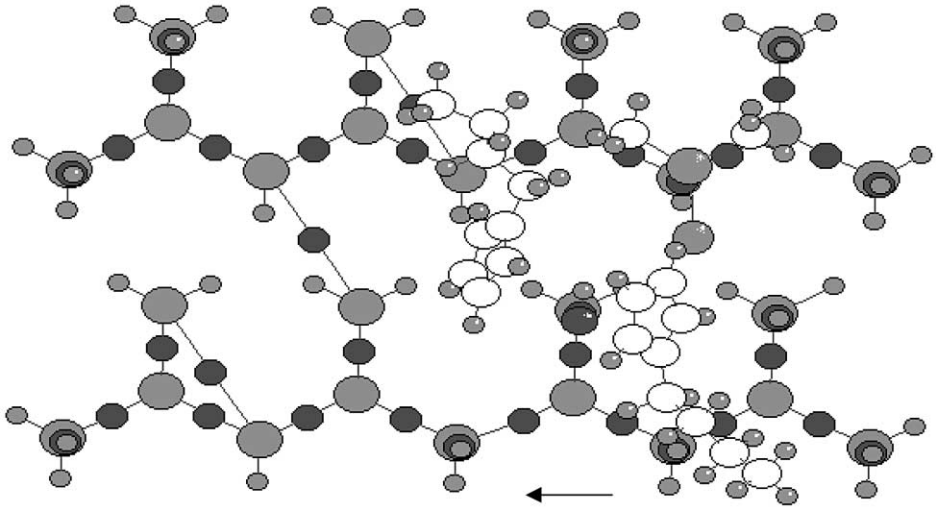

Fig. 17. Silica(1 1 1)–OZr(nBuCp)$_2$H$\cdots$Me$_2$ClSi–O–silica(1 1 1).

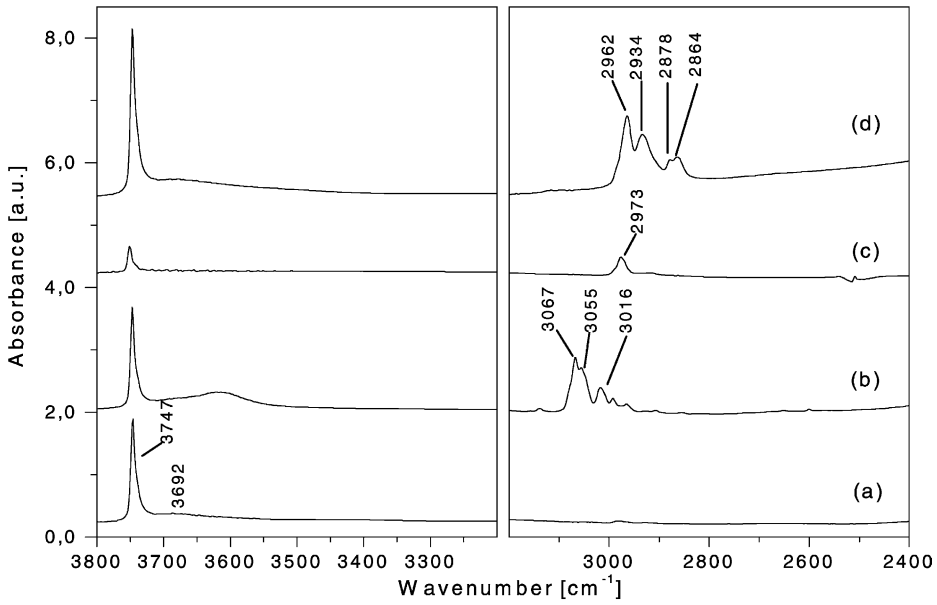

Fig. 18. IR spectra in the 3800–3300 and 3200–2400 cm^{-1} regions of: (a) SiO_2 dehydroxylated at 723 K for 16 h under vacuum; (b) same condition as in (a) followed by impregnation at 298 K with a 1.0 wt.% Si/SiO_2 methyldichloride solution of Ph_3SiCl; (c) same condition as in (a) followed by impregnation at 298 K with a 3.0 wt.% Si/SiO_2 methyldichloride solution of Me_3SiCl; and (d) same condition as in (a) followed by impregnation at 298 K with a 1.0 wt.% Si/SiO_2 methyldichloride solution of Me_2SiHCl, followed by impregnation at 298 K with a 0.12 wt.% Zr/SiO_2 toluene solution of $(n\text{BuCp})_2ZrCl_2$. The right hand side of the spectra is multiplied by a factor of 6.

Silica surface modified with 5.0 wt.% Si/SiO_2, using CH_3SiCl as modifier was also investigated by XPS in high-resolution mode in the O, Si and Cl regions. Table 1 reports XPS deconvolution parameters.

From the Si 2p spectrum, Si atoms in the sample bulk (103.4 eV) can be distinguished from those on the surface (101.8 eV). The species at high and low binding energies correspond, respectively, to 83 and 17% (see Table 4).

Two different O species were also detected: 532.1 and 529.1 eV, the latter corresponding to 13% of total area. The high BE signal can be attributed to silica oxygen, in an accordance with data reported in the literature for silica gel (532.5 eV) [29] and silica, crystobalite (532.5 eV) [30], for instance. The low BE species suggest the presence of an oxygen in a rich electronic environment.

The Cl 2p core level is constituted of a doublet corresponding to Cl $2p^{1/2}$ and Cl $2p^{3/2}$. In the present case, two different Cl species were detected, at approximately the same proportion. The one situated at 198.1/199.9 eV suggests chloride species in a more electronic environment, while the other one placed at 202.8/205.2 eV indicates more electron deficient ones.

The presence of these two Cl species can be related to O_3Si–Cl (from (1 1 1) plane) and $O_2SiMeCl$ (from

Table 4
XPS data from Si, O and Cl regions

Photoelectron	BE[a] (eV)	Relative elemental abundance (%)	FWHM[b] (eV)
Si 2p	103.4	83	2.3
	101.8	17	2.6
O 1s	532.1	87	2.5
	529.1	13	2.7
Cl 2p	198.1[c]	50	2.4
	199.9[d]		1.9
	202.8[c]	50	2.4
	205.2[d]		2.4

[a] Reference: Si 2p from SiO_2 (103.3 eV).
[b] Full width at half maximum intensity.
[c] Cl $2p^{1/2}$.
[d] Cl $2p^{3/2}$.

(1 0 0) plane). The presence of both of them in the same proportion can be related to the exchange of OH by Cl (known to occur in 15% of the surface following [25] — see Eq. 3). The presence of chlorine from the reaction of geminal groups (15% of the cristobalite surface — see Eq. 19) must be taken into account, too. The energies of both reactions are in the order. Another reaction that must be considered is the reaction Me_3SiCl with siloxanes, that generates the same O_3Si–Cl groups (1 1 1) plane (see Eq. 7). Certainly, the reactive siloxanes are present at low concentration. It is important to mention that 80 % of the total [OH] is consumed at the preparation step.

The XPS results permit us to verify the validity of the surface structure (85% (1 1 1) and 15% (1 0 0) because there are two kinds of Si (and O) at surface.

3.4. Ethylene polymerization

At the same nominal loading of organosilane (0.3 wt.% Si/SiO_2) the activity (in kg PE/mol Zr h bar units) decreases in the following order (see [8]):

Me_3SiCl (18) > Ph_3SiCl (15) > Me_2HSiCl (11)

Polymerization reaction was performed at 333 K, 1 atm, Al/Zr = 2000. The Zr content (wt.% Zr/SiO_2) decreases in the same way (0.6; 0.5; 0.12, respectively).

There are some reports about the possibility of the formation of an active site, being the support the counterion ($SiO^-Cp_2ZrMe^+$ cation 1 — low activity, low molecular weight) and perhaps another kind of sites, with MAO (coactivator) coordinated to the site, besides the surface (cation 2 — high activity, high molecular weight). These sites are difficult to form without external MAO because with supported Cp_2ZrCl_2 we need a coactivator and with supported Cp_2ZrMe_2 the possibilities of bimolecular deactivation and inactive site formation is high. If high amounts of organosilane avoid efficient coordination of MAO (cation 2), the lowering of activity and molecular weight is explained. If the direct impregnation leads to inactive sites by reaction with two isolated OH or binuclear cation formation in case of bare silica, it is easy to understand why Ph_3SiCl or Me_3SiCl are so excellent silica modifiers in terms of activity. The bimolecular deactivation of supported species is avoided, being the silane an horizontal spacer and the reaction with two OH from the surface is avoided in (1 1 1) planes, specially at high Me_3SiCl or Ph_3SiCl contents (see reactions 35–42, Table 2). There is an optimum Si content for both chemically modified silicas. This can be explained if we consider that the relation cation 1/cation 2 depends on the amount of supported organosilane. Higher amounts of these silanes avoid fixation of zirconocene/formation of the most active sites or even the monomer/MAO access is hindered. It is clear then that the polymer renders more homogeneous and the polydispersity is lower when the zirconocene is supported, especially with the series with higher amounts of supported organosilane. Molecular weight is higher than homogeneous one (in case of the optimum content of Ph_3SiCl — 0.3 wt.% Si/SiO_2) and is almost the same or decreases in case of the others silanes or higher amounts of Ph_3SiCl present.

With Me_2SiHCl at the same nominal content, the activity is lower, but the amount of supported zirconocene is rather low (0.12 versus 0.6 wt.% Zr/SiO_2). The FTIR results reported in reference [8] are in agreement with the results of the theoretical calculation.

The higher activity of the Me_3SiCl treated support can be related to the capacity of this silane to alkylate the zirconocene. This silane could provide a more acidic MAO at the active site formation step because of the exchange methyl (MAO)–chlorine (supported silane) (see reactions 26, 27 in Table 2 and reactions 44–49 in Table 3). However, the alkylation reaction is able to occur with the hydrogenorganosilane, too (see reaction 29 in Table 2 and reaction 33 in Table 3). In this case, the formation of Zr–H is possible (see reactions 28, 30 in Table 1 and reactions 31, 32, 34 in Table 3). The calculations performed with Me_3SiCl treated supports show that MAO can be chlorinated with the chlorine from the surface, especially if the chlorine concentration is high. Chlorinated MAO has probably higher acidity, and therefore, higher alkylating capacity, a fact reported by us in other paper [32]. The low $O_2SiMeCl$ relative to MAO concentrations (at the (1 0 0) plane only in SiO_2) avoids a stronger effect in activity. With Ph_3SiCl, the steric hindrance is very important to get the zirconocenes far from each other (see reaction 43, Table 3). In the case of higher amount of supported silane there is strong steric hindrance to the MAO/monomer to achieve the supported zirconocene and to generate an active site.

The low amount of zirconocene supported in case of Me_2HSiCl can be envisaged as a result of secondary reactions of the zirconocene with the silane. The supported zirconocene species would be mainly hydrogenated and/or alkylated, being easily activated by monomer, especially with the surface chlorine increasing the local acidity of MAO.

When we analyze the bare SiO_2, we can see that zirconocene is fixed with higher probability in the plane that leads to inactive sites (geminal or (1 0 0)). If we avoid this reaction through the modifier, the distribution of Zr will change and a higher amount of zirconocene would be placed on the (1 1 1) plane that leads to active sites. In this sense, Ph_3SiCl is located mainly on the (1 0 0) plane and its effect to avoid undesired species is more effective than the others (compare reaction 15 in Table 1 and reaction 24 in Table 2). This effect seems to be very important, despite of the lacking of the possibility of reaction of supported chlorine with MAO.

Perhaps a way to improve the activity is the chemical modification of the silica with two silanes: Ph_3SiCl and Me_3SiCl at low quantities.

Moroz et al. using Cp_2ZrMe_2 supported on SiO_2 found only traces of polyethylene. When the surface was treated with Me_3SiCl (being the ligand $SiMe_3$), the Zr amount decreases 20 times (from 0.32 to 0.014 mmol Zr/g) and the activity reaches 32 Kg PE/mol Zr h bar, without MAO, at 353 K, 10 bar, in *n*-hexane [31]. The impregnation procedure was similar to reference [8]. The extraction of the cited prepared catalyst with hexane containing 3% toluene, before use in reaction, decreases the amount of Zr from 0.13 to 0.04% and the activity achieves 304 Kg PE/mol Zr h bar. It seems that there are inactive soluble reaction products between the zirconocene and the silane that can be lowering the activity when remains strongly adsorbed on the surface. The low amount of zirconocene fixed in this case is due to the high treatment temperature with the silane (598 K). The amount of surface ligands is near 0.37 mmol/g (near 1.1% Si) in this work (real amount, no nominal). Their results can be explained because the lacking of reactive siloxanes due to the high-silica pre-treatment temperature (973 K) and the high real silane content, that efficiently can alkylate the zirconocene. Unfortunately, this paper does not report information about polyethylene characterization.

Acknowledgements

The authors want to acknowledge financial support from CONICET (Argentina) and FAPERGS (Brazil).

References

[1] D.H. Lee, Heterogeneization of metallocene catalysts for polymerization, in: T. Sano, T. Uozumi, H. Nakatani, M. Terano (Eds.), Progress and Development of Catalytic Olefin Polymerization, Technology and Education Publishers, Tokyo, 2000, pp. 137–146.
[2] H.T. Ban, T. Arai, C.-H. Ahn, T. Uozumi, K. Soga, Currents Trends Polym. Sci. 4 (1999) 47.
[3] M.R. Ribeiro, A. Deffieux, M.F. Portela, Ind. Eng. Chem. Res. 36 (1997) 1224.
[4] G.G. Hlatky, Chem. Rev. 100 (2000) 1347.
[5] J.H.Z. dos Santos, C. Krug, M.B. da Rosa, F.C. Stedile, J. Dupont, M.M. da Camargo Forte, J. Mol. Catal. A: Chem. 139 (1999) 199–207.
[6] J.H.Z. dos Santos, S. Dorneles, F.C. Stedile, J. Dupont, M.M. da Camargo Forte, I.J.R. Baumvol, Macromol. Chem. Phys. 198 (1997) 3529–3537.
[7] K. Soga, H.Y. Kim, T. Shiono, Macromol. Chem. Phys. 195 (1994) 3347–3360.
[8] J.H.Z. dos Santos, P.P. Greco, F.C. Stedile, J. Dupont, J. Mol. Catal. A: Chem. 154 (2000) 103–113.
[9] R. Hofmann, J. Chem. Phys. 39 (1963) 1392.
[10] G. Calzaferri, L. Forss, I. Kamber, J. Phys. Chem. 93 (1989) 5366.
[11] J. Sambeth, A. Juan, L. Gambaro, H. Thomas, J. Mol. Catal A: Chem. 118 (1997) 83.
[12] M.L. Ferreira, N. Castellani, D. Damiani, A. Juan, J. Mol. Catal. A. Chem. 122 (1997) 25.
[13] M.L. Ferreira, M. Volpe, J. Mol. Catal. A: Chem. 149 (1/2) (1999) 33–42.
[14] M.M. Branda, R. Montani, N. Castellani, Surf. Sci. 354 (1995) 295.
[15] M.L. Ferreira, M.M. Branda, A. Juan, D.E. Damiani, J. Mol. Catal. A: Chem. 122 (1997) 51–60.
[16] D.T. Mallin, M. Rausch, E. Mintz, A.L. Rheingold, J. Organomet. Chem. 381 (1990) 35–44.
[17] C. Kruger, M. Nolte, G. Erker, S. Thiele, Z. Naturforsch 47b (1992) 995–999.
[18] R.A. Howie, G.P. McQuillan, D.W. Thompson, G.A. Lock, J. Organomet. Chem. 303 (1986) 213–220.
[19] D.R. Lide (Ed.), Handbook of Chemistry and Physics, 76th Edition, CRC Press, Boca Raton, pp. 1995–1996.
[20] K.K. Unger, Porous silica, J. Chrom. Library 16 (1979).
[21] M.E. Bartram, T.A. Michalske, J.W. Rogers Jr., J. Phys. Chem. 95 (1991) 4453–4463.
[22] E.P. Talsi, N.V. Semikolenova, V.N. Panchenko, A.P. Sobolev, D.E. Babushkin, A.A. Shubin, V.A. Zakharov, J. Mol. Catal. A: Chem. 139 (1999) 131.
[23] I.Yu. Babkin, A.V. Kiselev, Russ. J. Phys. Chem. 36 (1962) 1326.

[24] A.V. Kiselev, V.I. Lygin, Infrared Spectra of Surface Compounds, Wiley, New York, 1975.
[25] M.L. Hair, W. Hertl, J. Phys. Chem. 75 (7) (1969) 2372–2378.
[26] M.L. Hair, Infrared Spectrocopy in Surface Chemistry, Marcel Dekker, New York, 1967.
[27] V.N. Pachenko, N.V. Semikolenova, I.G. Danilova, E.A. Paukhetis, V.A. Zakharov, J. Mol. Catal. A: Chem. 142 (1999) 27.
[28] L.J. Bellamy, The Infrared Spectra of Complex Molecules, Vol. 1, 3rd Edition, Chapman and Hall, Cambridge, 1975.
[29] V.I. Nefedov, Y.V. Salyn, G. Leonhardt, R. Scheibe, J. Electron. Spectrosc. Relat. Phenom. 10 (1977) 121.
[30] C.D. Wagner, D.E. Passoja, H.F. Hillery, T.G. Kinisky, H.A. Six, W.T. Jansen, J.A. Taylor, J. Vac. Sci. Technol. 21 (1982) 933.
[31] B.L. Moroz, N.K. Semikolenova, A.V. Nosov, V.A. Zakharov, S. Nagy, N. O'Reilly, J. Mol. Catal. A: Chem. 130 (1998) 121–129.
[32] M.L. Ferreira, P.G. Belelli, D.E. Damiani, Macromol. Chem. Phys., submitted for publication.